ChemComm

COMMUNICATION

View Article Online
View Journal

Cite this: DOI: 10.1039/d1cc03586j

Received 5th July 2021,
Accepted 16th August 2021

DOI: 10.1039/d1cc03586j

rsc.li/chemcomm

Red fluorescent zwitterionic naphthalenediimides with di/mono-benzimidazolium and a negatively-charged oxygen substituent†

Chunqin Wang,[a] Songyan Han,[a] Tianbao Wang,[a] Xuesong Zheng,[a] Linsen Zhou,[b] Yanhong Liu,[a] Cheng Zhang [a] and Ge Gao *[a]

The C–H/C–X cross-coupling of a benzimidazolium salt with 2Br-NDI afforded two unprecedented zwitterionic NDIs with di/mono-benzimidazolium and an extra negatively-charged oxygen substituent. They exhibited intensified red fluorescence in polar solvents and negative solvatochromism due to an intramolecular charge transfer process, and could specifically label lysosomes and the endoplasmic reticulum in living A549 cells, respectively. They represent a rare case of NDI-derived ionic fluorophores.

1,4,5,8-Naphthalenediimide and its derivatives (NDIs) are planar, electron deficient and π-conjugated molecules,[1] which have been extensively studied during the past decades due to their widespread application in the fields of optoelectronic devices,[2] chemical sensors,[3] organic dyes,[4] and bio-imaging.[5] Unmodified NDI generally has an absorption below 400 nm and weakly emits in the range of 400–450 nm.[6] While substitution on the diimide nitrogen atom shows limited influence on the optical and electrochemical properties of NDIs, profound impacts are found following core modification. For example, electron donating alkoxy and alkylamino groups substituted at the 2-, 3-, 6- and 7-positions significantly boost the fluorescence and bathochromically shift the emissions *via* intramolecular charge transfer (ICT).[7] Expansion of the π-conjugation by fusion with (hetero)aromatic rings can narrow the energy band gap and enhance π–π interactions, which may eventually improve the intermolecular charge transport for high performance organic field-effect transistors (OFETs).[8]

On the other hand, the introduction of electron withdrawing groups such as trifluoromethyl, cyano, sulfoxide and sulfone decreases the LUMO energy level, resulting in increased π-acidity and anion affinity.[9] More recently, NDIs with cationic functionalities have drawn much attention. Mukhopadhyay *et al.* reported the *in situ* synthesis of an extraordinarily stable radical cation of diphosphonium-substituted NDI.[10] This kind of NDI could be further reduced into air-stable, highly electron-rich doubly zwitterionic derivatives.[11] By replacement of one phosphonium moiety with an alkyl/aryl amino group, stable, high-SOMO zwitterionic radicals were obtained.[12] The same group later showcased that diviologen-modified NDIs could accept up to six electrons within a narrow window of about 1 V.[13] Tam and Wu *et al.* synthesized various dipyridinium-functionalized NDIs with different counter anions, and found interesting anion shuttling between the NDI core and the pyridinium moieties.[14] It needs to be pointed out that these cationic NDIs are not emissive.

Due to our continuous interests in ionic functional materials,[15] we previously used the imidazolium unit as an electron-withdrawing functionality to build a typical D–π–A fluorophore, which featured blue-colored aggregation-induced emission.[16] In 2018, we developed a Cu-catalyzed C–H/C–X cross-coupling reaction of imidazolium salts with aryl halides, by which a phenylene-bridged dibenzimidazolium compound was constructed to show electrochromic characteristics.[17] We therefore wanted to explore the unknown properties of electron deficient NDI-bridged dibenzimidazolium compounds synthesized using this method. To the best of our knowledge, no benzimidazolium-substituted NDI has been reported yet.[18] Herein, we would like to present the synthesis of two unexpected zwitterionic di/mono-benzimidazolium C-substituted NDIs with an extra negatively-charged oxygen substituent, which emit red fluorescence in polar solvents and specifically label different organelles in living cells.

Starting from a commercially available 1,4,5,8-naphthalenetetracarboxylic dianhydride (NDA), 2,6-dibromo-1,4,5,8-naphthalenetetracarboxylic dianhydride (2Br-NDA) was obtained by bromination using 1,3-dibromo-5,5-dimethylhydantoin (DBH) according to the literature procedure.[19] Subsequent condensation of 2Br-NDA with *n*-butylamine afforded the key intermediate 2Br-NDI in moderate yield (see the ESI†).[20] The C–H/C–X cross-coupling reaction of

[a] *Key Laboratory of Green Chemistry and Technology of Ministry of Education, College of Chemistry, Sichuan University, 29 Wangjiang Road, Chengdu 610064, P. R. China. E-mail: gg2b@scu.edu.cn*

[b] *Institute of Materials, China Academy of Engineering Physics, Mianyang 621907, P. R. China*

† Electronic supplementary information (ESI) available: Experimental procedures and characterization data. CCDC 2091134. For ESI and crystallographic data in CIF or other electronic format see DOI: 10.1039/d1cc03586j

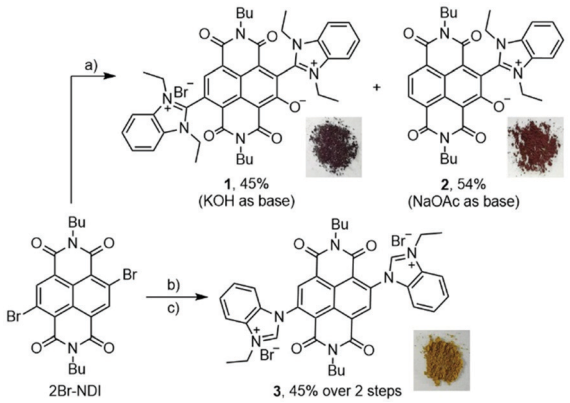

Scheme 1 Synthesis of compounds **1–3**. Conditions: (a) 2Br-NDI (0.1 mmol), 1,3-diethylbenzimidazolium bromide (0.3 mmol), Cu_2O (40 mol%), a base (0.3 mmol), and DMF (1 mL), N_2, 120 °C, 24 h; (b) 2Br-NDI (0.1 mmol), benzimidazole (0.4 mmol), Cu_2O (40 mol%), KOH (0.48 mmol), and DMSO (1 mL), N_2, 120 °C, 48 h; (c) bromoethane (0.5 mL) and acetonitrile (1 mL), 80 °C, 16 h. Insets: Photos of **1–3** in the solid state.

2Br-NDI with 1,3-diethylbenzimidazolium bromide under the catalysis of Cu_2O in the presence of a base provided two purple-colored spots on the TLC plates, which differed from the known cationic NDI derivatives. These two compounds were isolated, purified using column chromatography and characterized using NMR and high-resolution mass spectroscopy (HRMS). To our surprise, however, besides the designed mono- and dibenzimidazolium substitutions on the NDI core, a C–H oxygen substitution occurred next to the benzimidazolium moiety concomitantly, resulting in two zwitterionic NDI derivatives **1** and **2** (Scheme 1). **1** was a claret-colored solid with a metallic luster, while **2** was a rust-colored solid. In the ^{1}H NMR spectra, **1** showed a singlet at 8.39 ppm, corresponding to only one proton being left on the NDI core. For **2**, two doublets at 8.66 and 8.22 ppm are related to two adjacent protons on the NDI core, implying that debromination occurred. The HRMS analysis showed ion peaks at 739.3608 and 567.2600, respectively, which were in agreement with the structures of **1** (calcd $[M - Br^-]^+$: 739.3602) and **2** (calcd $[M + H]^+$: 567.2602). By varying the base used (Table S1, ESI†), the production of **1** and **2** could be tuned: as high as 54% yield of **2** was reached when sodium acetate was used, and **1** was only detected in a trace amount; when potassium hydroxide was employed, **1** was isolated in 45% yield accompanied by **2** in 11% yield. We did not find any compound without the extra oxygen substituent as we initially expected. For comparison, dibenzimidazolium N-substituted NDI **3** with no oxygen substituent was obtained *via* a sequential *N*-arylation and quarternization procedure (Scheme 1, for details, see the ESI†). **3** was a wheat-colored solid. It is noteworthy that heating 2Br-NDI or **3** alone in the absence of the benzimidazolium salt under otherwise identical conditions resulted in no reaction and recovery of the starting material, indicating a unique activating effect of the C-substituted benzimidazolium on the NDI core for oxygen substitution.

Single crystals of **2** were luckily obtained in a mixed solution of methanol, acetonitrile and ethyl acetate, and the structure was resolved using single crystal X-ray diffractometry as shown in Fig. 1. It is obvious to see the additional oxygen atom at the C3-position. No isolated counter anion was found in the crystal lattice, which unambiguously confirmed its zwitterionic structure. The bond length between C2 and C9 is 1.479 Å, which is within the range of a typical C–C single bond. The core NDI is not planar but slightly twisted. The dihedral angle between the benzimidazolium ring and the NDI plane is 85.1°, indicating very limited electron communication between these two units. The cationic benzimidazolium ring could probably only endow NDI with a pure electron-withdrawing inductive effect.

The optical properties of **1** and **2** were first studied in DMF (Fig. 2). Their DMF solutions were purple blue-colored and the UV-vis spectra similarly showed two absorption bands. The band in the UV area between 300–400 nm corresponds to the characteristic absorption of the NDI core.[1,6] The main band is bathochromically shifted into the visible region at around 580 nm, suggesting a strong ICT process. A shoulder peak emerges at lower wavelengths, presumably related to a vibronic fine structure in resonance with the naphthalenolate skeleton.[21] The molar extinction coefficient (ε) of **2** is 36 400 M^{-1} cm^{-1}, which is about three times larger than that of **1** (12 000 M^{-1} cm^{-1}). **1** and **2** both emitted red fluorescence with maximum emissions at 655 and 641 nm, respectively. The quantum yield of **2** was measured to be 3.0%, while **1** showed a lower value of 0.35%, which is probably due to more nonradiative decay arising from one more benzimidazolium substituent. The similar spectra of **1** with a bromide anion and **2** without a counter anion suggested that there is no anion–π interaction between the NDI core and the bromide anion.

Compounds **1** and **2** were soluble in common polar solvents such as chloroform, ethyl acetate, acetonitrile, acetone, dimethyl sulfoxide, and methanol, *etc.* Furthermore, **1** could even be dissolved in water (Fig. S1, ESI†). A negative solvatochromism[22] was observed (Fig. S2, S3 and Table S3, ESI†). The maximum absorption of **1** was hypochromically shifted 63 nm from 604 nm in dichloromethane to 541 nm in water, while a 47 nm shift was recorded for **2** from 583 nm in dichloromethane to 539 nm in methanol. These zwitterionic molecules were expected to be stabilized by polar solvents, resulting in a lowered HOMO energy as well as an enlarged HOMO–LUMO gap, which eventually led to hypochromic shifts of the absorption. Although the emissions were less shifted by variation of the solvent, the intensities were enhanced with the

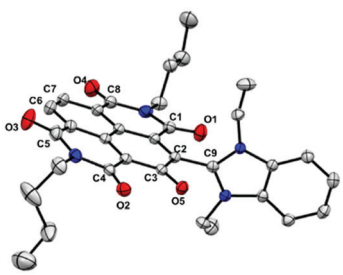

Fig. 1 ORTEP drawing with ellipsoids drawn at the 50% level for **2**. The hydrogen atoms are omitted for clarity.

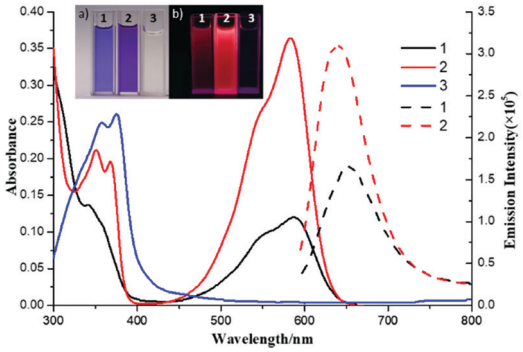

Fig. 2 UV-vis (solid lines) and emission spectra (dotted lines) of **1** and **2** (1×10^{-5} M) in DMF at r.t. The absorption of compound **3** was measured in methanol. Insets: Photos of solutions of **1–3** under (a) ambient light and (b) 365 nm irradiation.

increase of solvent polarity. The quantum yield of **1** in water was enhanced about 10 times compared to that in DMF to 3.42%, and that of **2** in MeOH was enhanced about 2 times to 6.43%. This phenomenon is in contrast to that observed for alkylamino-substituted NDI fluorophores, which exhibit considerably diminished fluorescence in protic solvents.[7a] The optical property of the reference compound **3** was measured in methanol because it decomposed slowly in DMF. The methanol solution was almost colorless and its absorption spectrum exhibited only one absorption band in the UV region, which is attributed to the NDI core. **3** emitted no fluorescence at all.

Cyclic voltammetry (CV) was then conducted to measure the energy levels of **1–3** (Fig. S4, S5 and Tables S4, S5, ESI†). **1** and **2** showed two reversible reduction peaks during the cathodic sweep, and no oxidation peak was observed during the anodic sweep. The first reduction potential of **1** was more positive than that of **2**. The LUMO energy levels of **1** and **2** were determined to be −3.89 and −3.60 eV from the $E_{1/2}$ values of the first reduction potentials using the equation: $E_{LUMO} = -4.80\ eV - E_{red1}$. The HOMO energy levels were calculated to be −5.86 and −5.57 eV according to the equation: $E_{HOMO} = E_{LUMO} - E_g$, wherein E_g was estimated from the edge of the absorption maximum. In comparison with the LUMO (−3.83 eV) and HOMO (−7.01 eV) of the parent NDI, the HOMO energy levels are significantly elevated while the LUMO energy levels are less affected. However, the LUMO of **2** is raised by 0.23 eV. These results suggested that the negatively charged oxygen atom exerts a more profound electron-donating influence on the NDI core than the electron-withdrawing effect of the benzimidazolium moieties, in line with the bathochromically-shifted absorption and red-light emission properties of **1** and **2**. In the absence of an electron-donating moiety, the LUMO of **3** is significantly lowered as predicted (see the ESI†).

To further understand the optical properties of **1–3**, DFT calculations at the B3LYP/6-31g(d,p) level were performed and the molecular orbital (MO) distributions are shown in Fig. S6 (ESI†). The HOMO/LUMO energies of **1** and **2** were calculated to be −5.90/−3.35 and −5.80/−2.96 eV (Fig. S7, ESI†), respectively, which are in accordance with the measurements. The DFT-optimized structures revealed that the dihedral angles between the C-substituted benzimidazolium moiety and the NDI plane were 83° and 85°, respectively (Fig. S8, ESI†), which is consistent with the single crystal structure of **2**. Their HOMOs and LUMOs are therefore mainly located on the NDI skeleton and the oxygen substituent with a small separation, suggesting an ICT process from the oxygen substituent to the NDI core. The similar MO distributions of **1** and **2** explain their similar optical spectra. The DFT-optimized geometry of **3** disclosed a 61° dihedral angle between the N-substituted benzimidazolium moiety and the NDI plane, leading to the distribution of the HOMO mainly on the benzimidazolium moiety and the LUMO on the NDI skeleton (Fig. S7 and S8, ESI†). Therefore, the unique red fluorescence of **1** and **2** originates from the ICT process between the strongly electron-donating negatively-charged oxygen atom and the NDI core without any contribution from the C-substituted benzimidazolium moieties. In compound **3**, the two N-substituted benzimidazolium moieties served as typical electron-withdrawing groups through the resonated and positively-charged nitrogen atoms, quenching the inherently very weak fluorescence of the NDI core.

Time-dependent density functional theory (TD-DFT) calculations were performed at the optimally tuned PBE1PBE/6-31g(d,p) level of theory on the above optimized geometries of **1–3**. The maximum absorption of **1** at 587 nm was characterized by HOMO → LUMO (S_2, 558 nm, oscillator strength $f = 0.2384$). The absorption of **2** at 583 nm was attributed to HOMO → LUMO (S_2, 548 nm, $f = 0.2277$). However, the HOMO → LUMO transition is prohibited in **3** ($f < 0.01$). A large contribution from the HOMO−4 → LUMO transition and a small contribution from the HOMO−8 → LUMO transition (S_{16}, 368 nm, $f = 0.2799$) were responsible for its absorption at 375 nm.

The red fluorescence in highly polar solvents of ionic **1** and **2** implied potential applications as biomarkers in living cell labelling, taking advantage of the low cell damage by visible-light excitation, the low interference from background fluorescence and the good membrane penetrating ability.[15e,23] Hence, the fluorescence imaging capabilities of **1** and **2** were evaluated in A549 cells. The cells were cultivated with **1** in PBS and with **2** in PBS containing 1% DMSO for 15 minutes at 37 °C, respectively. The cell labelling status was viewed under a confocal microscope to show that both **1** and **2** penetrated and labeled the A549 cells with red fluorescence (Fig. S9 and S10, ESI†). The morphological distribution of the fluorescence suggested that **1** might gather in the lysosomes, while **2** might be located in the endoplasmic reticulum (ER). Co-staining experiments using commercially available Lyso-Tracker Green and ER-Tracker™ Green were subsequently conducted, respectively. As seen in Fig. 3, the images from the red fluorescence channel overlapped well with images from the green fluorescence channel, and the Pearson's coefficient values were calculated to be 0.93 and 0.91 accordingly (Table S9, ESI†). Moreover, the cytotoxicities of **1** and **2** were also examined using MTS (CellTiter 96 AQueous One Solution Cell Proliferation Assay) (Fig. S11, ESI†). **1** and **2** showed low cytotoxicities as the cell viability was about 80% at a concentration of 4 μM. These results demonstrated the specific fluorescent labelling ability of **1** and **2** towards different organelles in living cells.

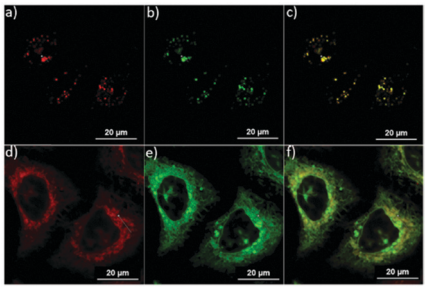

Fig. 3 Fluorescent images of A549 cells stained with (a) **1** (1.0 μM, λ_{ex} = 543 nm, λ_{em} = 600–700 nm) and (b) Lyso-Tracker Green (1.0 μM, λ_{ex} = 488 nm, λ_{em} = 500–600 nm); (c) merged image of (a) and (b); fluorescent images of A549 cells stained with (d) **2** (1.0 μM, λ_{ex} = 543 nm, λ_{em} = 600–700 nm) and (e) ER-Tracker™ Green (1.0 μM, λ_{ex} = 488 nm, λ_{em} = 500–600 nm); (f) merged image of (d) and (e).

In summary, we have synthesized for the first time two zwitterionic NDIs with electron-withdrawing di-/mono-benzimidazolium moieties and an extra electron-donating negatively-charged oxygen substituent. They have similar LUMO levels and significantly elevated HOMO levels in comparison with the parent NDI, suggesting a larger impact of the later. They not only exhibit unusual enhanced red fluorescence in polar solvents and negative solvatochromism, but also specifically label lysosomes and the endoplasmic reticulum, respectively. These dual functional NDIs are of interest for further investigation.

Financial support from the National NSF of China (No. 21772134) and the Fundamental Research Funds for the Central Universities (No. 20826041D4117) is gratefully acknowledged.

Conflicts of interest

There are no conflicts to declare.

Notes and references

1 (*a*) N. Sakai, J. Mareda, E. Vauthey and S. Matile, *Chem. Commun.*, 2010, **46**, 4225; (*b*) S. Kumar, J. Shukla, Y. Kumar and P. Mukhopadhyay, *Org. Chem. Front.*, 2018, **5**, 2254; (*c*) J. Shukla and P. Mukhopadhyay, *Eur. J. Org. Chem.*, 2019, 7770; (*d*) C. Li, Z. Lin, Y. Li and Z. Wang, *Chem. Rec.*, 2016, **16**, 873.
2 (*a*) H. E. Katz, A. J. Lovinger, J. Johnson, C. Kloc, T. Siegrist, W. Li, Y.-Y. Lin and A. Dodabalapur, *Nature*, 2000, **404**, 478; (*b*) X. Zhan, A. Facchetti, S. Barlow, T. J. Marks, M. A. Ratner, M. R. Wasielewski and S. R. Marder, *Adv. Mater.*, 2011, **23**, 268.
3 S. Maniam, H. F. Higginbotham, T. D. M. Bell and S. J. Langford, *Chem. – Eur. J.*, 2019, **25**, 7044.
4 S. Maniam, H. F. Higginbotham, S.-X. Guo, T. D. M. Bell, E. I. Izgorodina and S. J. Langford, *Asian J. Org. Chem.*, 2014, **3**, 619.
5 D. Filippo, F. Marco, G. Vincenzo, C.-R. Graziella, Z. Nadia and F. Mauro, *Org. Biomol. Chem.*, 2015, **13**, 570.
6 D. Gosztola, M. P. Niemczyk, W. Svec, A. S. Lukas and M. R. Wasielewski, *J. Phys. Chem. A*, 2000, **104**, 6545.
7 (*a*) F. Würthner, S. Ahmed, C. Thalacker and T. Debaerdemaeker, *Chem. – Eur. J.*, 2002, **8**, 4742; (*b*) C. Thalacker, C. Röger and F. Würthner, *J. Org. Chem.*, 2006, **71**, 8098; (*c*) C. Röger and F. Würthner, *J. Org. Chem.*, 2007, **72**, 8070.
8 (*a*) S. Katsuta, K. Tanaka, Y. Maruya, S. Mori, S. Masuo, T. Okujima, H. Uno, K.-I. Nakayamabe and H. Yamada, *Chem. Commun.*, 2011, **47**, 10112; (*b*) W. Yue, J. Gao, Y. Li, W. Jiang, S. D. Motta, F. Negri and Z. Wang, *J. Am. Chem. Soc.*, 2011, **133**, 18054; (*c*) K. Cai, Q. Yan and D. Zhao, *Chem. Sci.*, 2012, **3**, 3175; (*d*) J. Gao, Y. Li and Z. Wang, *Org. Lett.*, 2013, **15**, 1366; (*e*) J. Li, Y.-H. Hu, C.-W. Ge, H.-G. Gong and X.-K. Gao, *Chin. Chem. Lett.*, 2018, **29**, 423.
9 (*a*) B. A. Jones, A. Facchetti, M. R. Wasielewski and T. J. Marks, *J. Am. Chem. Soc.*, 2007, **129**, 15259; (*b*) J. Chang, Q. Ye, K.-W. Huang, J. Zhang, Z.-K. Chen, J. Wu and C. Chi, *Org. Lett.*, 2012, **14**, 2964; (*c*) V. V. Roznyatovskiy, D. M. Gardner, S. W. Eaton and M. R. Wasielewski, *Org. Lett.*, 2014, **16**, 696; (*d*) Y. Kumar, S. Kumar, K. Mandal and P. Mukhopadhyay, *Angew. Chem., Int. Ed.*, 2018, **57**, 16318.
10 (*a*) S. Kumar, M. R. Ajayakumar, G. Hundal and P. Mukhopadhyay, *J. Am. Chem. Soc.*, 2014, **136**, 12004; (*b*) S. Kumar and P. Mukhopadhyay, *Green Chem.*, 2018, **20**, 4620.
11 S. Kumar, J. Shukla, K. Mandal and P. Mukhopadhyay, *Chem. Sci.*, 2019, **10**, 6482.
12 J. Shukla, S. Kumar, Rustam and P. Mukhopadhyay, *Org. Lett.*, 2020, **22**, 6229.
13 J. Shukla, M. R. Ajayakumar, Y. Kumar and P. Mukhopadhyay, *Chem. Commun.*, 2018, **54**, 900.
14 T. L. D. Tam, C. K. Ng, X. Lu, Z. L. Lim and J. Wu, *Chem. Commun.*, 2018, **54**, 7374.
15 (*a*) S. Yang, J. You, J. Lan and G. Gao, *J. Am. Chem. Soc.*, 2012, **134**, 11868; (*b*) H. Zhou, Y. Zhao, G. Gao, S. Li, J. Lan and J. You, *J. Am. Chem. Soc.*, 2013, **135**, 14908; (*c*) J. Tang, S. Li, Z. Liu, Y. Zhao, Z. She, V. D. Kadam, G. Gao, J. Lan and J. You, *Org. Lett.*, 2017, **19**, 604; (*d*) Z. She, Y. Wang, D. Wang, Y. Zhao, T. Wang, X. Zheng, Z.-X. Yu, G. Gao and J. You, *J. Am. Chem. Soc.*, 2018, **140**, 12566; (*e*) V. D. Kadam, B. Feng, X. Chen, W. Liang, F. Zhou, Y. Liu, G. Gao and J. You, *Org. Lett.*, 2018, **20**, 7071.
16 C. Gao, G. Gao, J. Lan and J. You, *Chem. Commun.*, 2014, **50**, 5623.
17 S. Li, J. Tang, Y. Zhao, R. Jiang, T. Wang, G. Gao and J. You, *Chem. Commun.*, 2017, **53**, 3489.
18 A zwitterionic imidazolium substituted perylene bisimide radical was reported, see: D. Schmidt, D. Bialas and F. Würthner, *Angew. Chem., Int. Ed.*, 2015, **54**, 3611.
19 A. Sarkar, S. Dhiman, A. Chalishazar and S. J. George, *Angew. Chem., Int. Ed.*, 2017, **56**, 13767.
20 Y. Matsunaga, K. Goto, K. Kubono, K. Sako and T. Shinmyozu, *Chem. – Eur. J.*, 2014, **20**, 7309.
21 A. Schade, R. Menzel, H. Görls, S. Spange and R. Beckert, *Asian J. Org. Chem.*, 2013, **2**, 498.
22 (*a*) A. V. Kulinich, E. K. Mikitenko and A. A. Ishchenko, *Phys. Chem. Chem. Phys.*, 2016, **18**, 3444; (*b*) A. Morimoto, Y. Hayashi, T. Maeda and S. Yagi, *Dyes Pigm.*, 2021, **184**, 108768.
23 (*a*) N. Jiang, J. Fan, F. Xu, X. Peng, H. Mu, J. Wang and X. Xiong, *Angew. Chem.*, 2015, **127**, 2540; (*b*) Y. Cheng, G. Li, Y. Liu, Y. Shi, G. Gao, D. Wu, J. Lan and J. You, *J. Am. Chem. Soc.*, 2016, **138**, 4730; (*c*) X. Chen, L. Yan, Y. Liu, Y. Yang and J. You, *Chem. Commun.*, 2020, **56**, 15080; (*d*) S. Zhang, H. Lia, Q. Yao, S. Ghazalia, J. Fan, J. Du, J. Wang, F. Gao, M. Li, H. Wang, C. Dong and X. Peng, *Chin. Chem. Lett.*, 2020, **31**, 2913.

